Université de Mons
Faculté Polytechnique – Service de Mécanique Rationnelle, Dynamique et Vibrations
31, Bld Dolez - B-7000 MONS (Belgique)
065/37 42 15 – georges.kouroussis@umons.ac.be

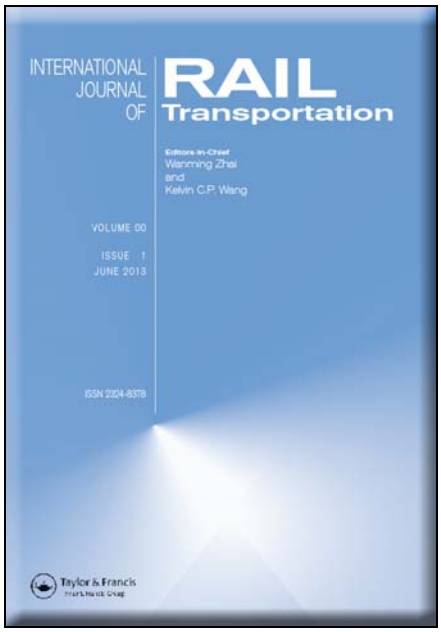

B. Olivier, O. Verlinden, G. Kouroussis, A vehicle/track/soil model using co-simulation between multibody dynamics and finite element analysis, *International Journal of Rail Transportation*, 8(2): 135–158, 2020.

INTERNATIONAL JOURNAL OF RAIL TRANSPORTATION
2020, VOL. 8, NO. 2, 135–158
https://doi.org/10.1080/23248378.2019.1642152

Taylor & Francis
Taylor & Francis Group

A vehicle/track/soil model using co-simulation between multibody dynamics and finite element analysis

Bryan Olivier, Olivier Verlinden and Georges Kouroussis

Department of Theoretical Mechanics, Dynamics and Vibrations, Université de Mons — UMONS, Mons, Belgium

ABSTRACT

Due to the always growing computing power, virtual models become nowadays a popular mean to simulate complex problems such as vehicle stability, track settlement or ground-borne vibrations induced by railway vehicles. This paper presents a co-simulation model of a vehicle passing on a track that lays on a soil. The model is split into two subsystems that are the vehicle and track subdomains and the soil subdomain. The coupled vehicle/track subsystem is modeled into an in-house multibody dedicated software package while the soil is entirely modeled with the help of a finite element analysis software. The results obtained using Jacobi and Gauß-Seidel methods, two different co-simulation techniques, will be compared to an already validated two-step model. Moreover, besides the results, this paper presents the coupling technique used between both subsystems to allow co-simulation and depicts the data management between the two distinct simulation environments.

ARTICLE HISTORY
Received 3 April 2019
Revised 3 July 2019
Accepted 7 July 2019

KEYWORDS
Solver-coupling; multibody simulation; co-simulation; soil dynamics; railway; finite element analysis

1. Introduction

In railway dynamics, there exist models or virtual prototypes focused on the vehicle dynamics. Those models can be, for example, dedicated to the characterization of the vehicle performance in a specific situation [1]. It can also provide the motion of a car containing passengers in order to prevent any discomfort due to an undesirable motion. In all cases, railway vehicles are complex structures involving a substantial number of bodies, suspension elements linking those bodies and then many relative motions. This kind of mechanical system is usually modeled using multibody dynamics techniques. Besides its own dynamics, the vehicle is usually rolling over a track that lays on a soil. When focusing on vehicle dynamics, the motion of the soil is frequently neglected since its effect remains small in comparison with the vehicle motion or the track motion in mid- and high-frequency. This effect is higher but still limited in low frequency [2]. Moreover, in terms of their mathematical representation, the vehicle, the track and the soil are clearly different structures. Indeed, the vehicle involves a limited number of equations of motion depending on the number of degrees of freedom used to represent

CONTACT Bryan Olivier bryan.olivier@umons.ac.be Department of Theoretical Mechanics, Dynamics and Vibrations, Université de Mons — UMONS, Place du Parc 20, Mons B-7000, Belgium

the motion of the bodies, usually supposed to be rigid, constituting the entire vehicle. Meanwhile, the track and the soil are continuous and flexible structures that are commonly represented using finite element techniques. Since the accuracy of a finite element representation of a structure directly depends on the number of elements taken into account, the number of degrees of freedom involved is much higher than in a rigid multibody representation.

During the last decades, specific numerical solvers [3–5] were developed for specific sets of equations. However, each solver remains suited for particular equations sets. This means that in a multiphysics model, such as the vehicle/track/soil model treated in this paper, it is common that different parts require solvers enjoying different properties, making it difficult to find an appropriate solver if a monolithic model is considered. In the railway domain, the vehicle/track/soil interaction was already studied through three-dimensional models [6–8] and two-step models were developed [9–15] in order to break down the monolithic model into parts such that each part can use its own adapted numerical solver. However, since the parts are integrated sequentially, the coupling between the parts is commonly insured by including, in each part, a reduced version of the other parts.

Contrarily to two-step models (Figure 1(a)), this paper presents a coupling of the vehicle/track/soil parts during the process of numerical integration. Similar studies are available in the literature and focus on the vehicle/track dynamics [16–19]. Generally speaking, the developed models focus on vehicle dynamics and realize the coupling between a multibody modeling of the vehicle and a finite element modeling of the track at the wheel/rail contact. The aim followed is usually the possibility to provide a simulation that can run in parallel. The model presented in this paper also deals with the vehicle/track dynamics but takes the soil into account. Moreover, it is split into two parts that are the vehicle/track and soil subsystems and each subsystem is defined and numerically solved within its environment (Figure 1(b)). Indeed, the vehicle and track subsystem is modeled

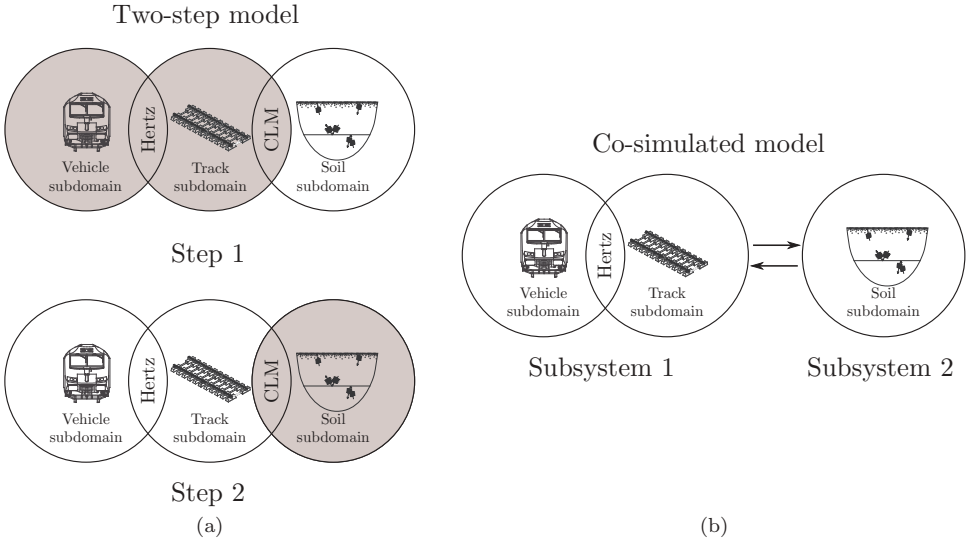

Figure 1. From the two-step model (a) to co-simulation (b).

and time-integrated using an in-house multibody dedicated software called EasyDyn [20] while the soil is modeled and time-integrated using the commercial finite element software ABAQUS [21]. Moreover, different methods of data management are investigated with the co-simulated model built for which a sequential and a parallel coupling schemes, denoted Gauß-Seidel and Jacobi respectively, will be presented and examined. Furthermore, in opposition to two-step models, the so-called co-simulated model does not require a reduced modeling of the other parts in each subsystem. However, since both subsystems are time-integrated simultaneously, a communication between them is required during the integration process. This process management and data exchange will be performed thanks to a TCP/IP server/client communication between both simulation environments.

2. Reference two-step model

The validation of the vehicle/track/soil model involving co-simulation is proposed by the comparison with the two-step model proposed by Kouroussis et al. [22]. As depicted in Figure 1, this two-step model is composed of three different subdomains dispatched into two distinct parts. The reference two-step and the co-simulated modelings differ only by the coupling technique used, without changing the nature of each subdomain. The three different subdomains are:

- The vehicle subdomain: modeled using the minimal coordinates approach in multibody dynamics. It can be any railway related vehicle from a complete train to a simple wheelset. For the sake of simplicity, the vehicle considered in the present case is a single wheel.
- The track subdomain: composed of the rails, the railpads, the sleepers and the ballast all the subballast structure is included in the general term ballast). The rails are modeled using a regular finite element representation through Euler-Bernoulli beam elements while the sleepers are considered as simple lumped masses animated with a vertical motion. In particular, each sleeper has then one degree of freedom while each node of the finite element modeling of the rail has two degrees of freedom, one for the vertical motion and one for the rotation in a planar case. Since the railpads and the ballast are considered in the track, the choice to model them as uncoupled spring and damper systems was made (similar to the situation depicted in Figure 2).
- The soil subdomain: modeled with an hemi-spherically shaped finite element model. The soil is split into a finite element meshed kernel, on which the track lays, and a semi-infinite element wrapping tied to the kernel.

The two steps involved in this reference model are defined below.

- Firstly, the vehicle and the track subdomains are time-integrated in order to compute the forces applied by the sleepers on the soil. Those forces are directly applied through the ballast located between the ground (soil surface) and the sleepers. In order to provide the best estimation of the track/soil forces, a reduced Coupled Lumped Masses (CLM) model [23] of the soil is added such that the vertical and longitudinal waves propagating through the soil are taken into account. This computation is performed using EasyDyn.

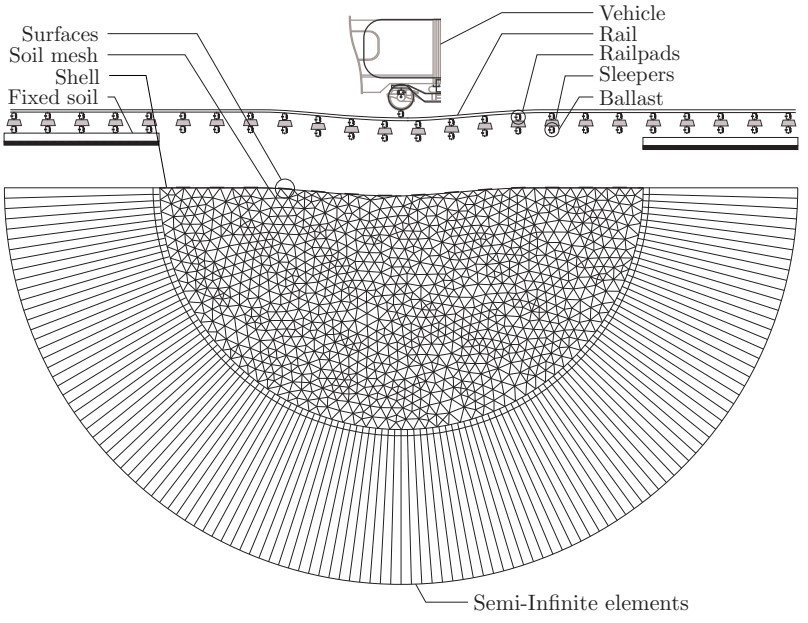

Figure 2. Representation of the displacement/force co-simulated vehicle/track/soil model coupled at the ballast level.

- Secondly, the forces obtained in the first step are applied on the soil modeling implemented in ABAQUS.

Following the aforementioned two steps, it can be deduced that the motion of the soil modeled in the second step does not directly affect the values of the forces going through the ballast. Indeed, due to the sequential character of the two-step model, there is no feedback of the soil step in the vehicle/track/CLM step. Therefore, the CLM modeling of the soil should be as accurate as possible and may be defined iteratively. As depicted in Figure 1, the interest of the co-simulated model presented in this paper lays on the complete coupling between the soil motion and the track motion. Moreover, the CLM representation of the soil is no more necessary since the coupling is directly made during the process of coupled time integration.

3. Displacement/force co-simulated model

The construction of the model including co-simulation follows the same structure as the previously presented two-step model. Indeed, the subdomains remaining identical for comparison purposes, the co-simulated model illustrated in Figure 2 involves two different subsystems that almost correspond to the two parts of the reference model. They are defined as follow.

- **Subsystem 1** involves the vehicle and track subdomains. Since the motion of the sleepers is now directly coupled to the motion of the soil through the mechanism of co-simulation, no additional reduced representation of the soil (such as the CLM soil

reduction) is required. This part is represented on top of Figure 2 and includes the vehicle, the rail, the sleepers, and also the railpads and the ballast as coupling elements.

- **Subsystem 2** consists of the soil, identically to the second step of the reference model. The difference lays on the definition of the forces acting on the soil that are updated during the coupled time-integration process.

3.1. Vehicle/track subsystem

The vehicle/track subsystem is represented by three sets of equations corresponding to the vehicle subdomain and the two distinct components of the track subdomain: the rail and the sleepers. The general set of equations is detailed in Equation (1). It has to be mentioned that the entire vehicle/track subsystem is defined in two dimensions since the problem is symmetrical along the longitudinally vertical plane. Therefore, for this subsystem, only the longitudinal-vertical plane motions are considered. Because of this two-dimensional characteristic, the total number of degrees of freedom of this subsystem can significantly be reduced.

Even if the vehicle is, in the present work, a simple wheelset with only one degree of freedom, Equation (1a) describes the general equation obtained through a multibody representation of a vehicle. This set of n_v equations, where n_v represents the number of configuration parameters $\mathbf{q}_v$ describing the vehicle motion, is divided in three terms: a $\mathbf{M}_v$ matrix containing the inertia information, a $\mathbf{h}_v$ vector representing the centrifugal, gyroscopic and Coriolis contributions and a vector $\mathbf{g}_v$ containing the internal and external applied forces on the vehicle system. Using EasyDyn, this set of equations is automatically and symbolically established thanks to the kinematic description of the multibody system through homogeneous transformation matrices [20].

Meanwhile, the track subdomain contains the rail and the sleepers respectively described by Equation 1(b,c). Thanks to an Euler-Bernoulli beam (finite element) representation of the rail, a set of n_r equations in terms of the n_r degrees of freedom $\mathbf{q}_r$ is obtained. $\mathbf{M}_r$ and $\mathbf{K}_r$ are the mass and stiffness matrices corresponding to the rail elements respectively. The continuous rail is split into elements with 2 nodes and 4 degrees of freedom. Indeed, each node has a vertical degree of freedom as well as a rotational degree of freedom about a direction perpendicular to the plane of motion. As it can be seen in Equation (1b), no damping is considered in the finite element representation of the rail since it is supposed to be negligible with respect to the material damping of the railpads and the ballast. The sleepers are here considered as lumped masses moving vertically such that the matrix $\mathbf{M}_s$ is a diagonal matrix in which each diagonal term represents the mass of a sleeper. Through this definition, the sleepers equation set (1c) involves n_s equations in terms of the n_s vertical degrees of freedom $\mathbf{q}_s$. In both (1b) and (1c) Equations, the $\mathbf{g}_r$ and $\mathbf{g}_s$ terms represent the rail and sleepers weights respectively.

$$\mathbf{M}_v(\mathbf{q}_v)\ddot{\mathbf{q}}_v + \mathbf{h}_v(\mathbf{q}_v, \dot{\mathbf{q}}_v) - \mathbf{g}_v(\mathbf{q}_v, \dot{\mathbf{q}}_v, t, \mathbf{f}_{\text{rail/wheel}}) = 0 \tag{1a}$$

$$\mathbf{M}_r\ddot{\mathbf{q}}_r + \mathbf{K}_r\mathbf{q}_r - \mathbf{W}_r\mathbf{f}_{\text{wheel/rail}} - \mathbf{f}_{\text{sleepers/rail}} - \mathbf{g}_r = 0 \tag{1b}$$

$$\mathbf{M}_s\ddot{\mathbf{q}}_s - \mathbf{f}_{\text{rail/sleepers}} - \mathbf{f}_{\text{soil/sleepers}} - \mathbf{g}_s = 0 \tag{1c}$$

The $\mathbf{f}_{\text{rail/wheel}}$ and $\mathbf{f}_{\text{sleepers/rail}}$ terms involved in Equation (1) insure the coupling between the three distinct sets of equations. Depending, on the number of contact points n_c, $\mathbf{f}_{\text{rail/wheel}}$ is a vector of length n_c containing the elastic forces developed between the wheels and the rail and defined using a linear contact theory. Since the rail is discretized, the wheel/rail contact force vector $\mathbf{f}_{\text{rail/wheel}}$ is multiplied by a matrix $\mathbf{W}_r$ containing shape functions [24]. This insures that the force vector is transformed into an appropriate vector of forces and torques, applied on the nodes of the rail elements on which the wheels are, in the track subdomain. Moreover, these shape functions are also used to compute the vertical displacement of the rail at the exact axial positions of the wheels using the displacements and rotations of the nodes of the element on which the wheel is passing over.

The coupling between the sleepers and the rail is performed by the railpads that are considered as linear spring-dashpot elements with stiffness and damping coefficients denoted k_p and d_p respectively. However, since there possibly exist more than one element of rail between two sleepers, only certain nodes of the rail are involved in the rail/sleepers coupling.

As for the railpads, the ballast is considered as a bunch of spring-damper elements of stiffness k_b and damping d_b coefficients. However, it is remarked on Figure 2 that the coupling is performed at the ballast level. It is also remarked that the vehicle/track subsystem is longitudinally divided into three parts. The middle part concerns its coupling with the soil subsystem while the external parts are fixed in the vehicle/track subsystem and do not exist in the soil subsystem. If the coupling will be detailed further in this paper, the existence of the fixed part in the present subsystem simplifies the determination of the initial configuration, corresponding to the static equilibrium position of the vehicle/track subsystem.

The numerical solver used to time-integrate the equations of motion in EasyDyn is an implicit Newmark-β scheme [3] with integration parameters $\beta = 0.25$ and $\gamma = 0.5$ such that the spectral radius is unitary and it does not add numerical damping to the results [25]. Moreover, the internal timestep is adaptive in order to improve the convergence of the algorithm.

3.2. Soil subsystem

The soil subsystem is entirely modeled using a finite element approach developed by Kouroussis et al. [22] in the ABAQUS commercial software. Contrarily to the vehicle/track subsystem, the soil is modeled as a three-dimensional hemispherical structure. The final purpose of this design is to estimate the level of ground-borne vibrations generated by a running train. Therefore, the three-dimensional character of the soil provides information on the vibrations with respect to the distance from the track. Several features such as a specific soil (or ground) configuration or the presence of a building close to the track could even be taken into account in the end.

As depicted in Figures 2 and 3, the soil modeling is composed of two different parts:

- The kernel: it consists of a solid hemisphere meshed with tetrahedral elements. Two tracks lay on the top surface of this kernel, placed symmetrically with respect

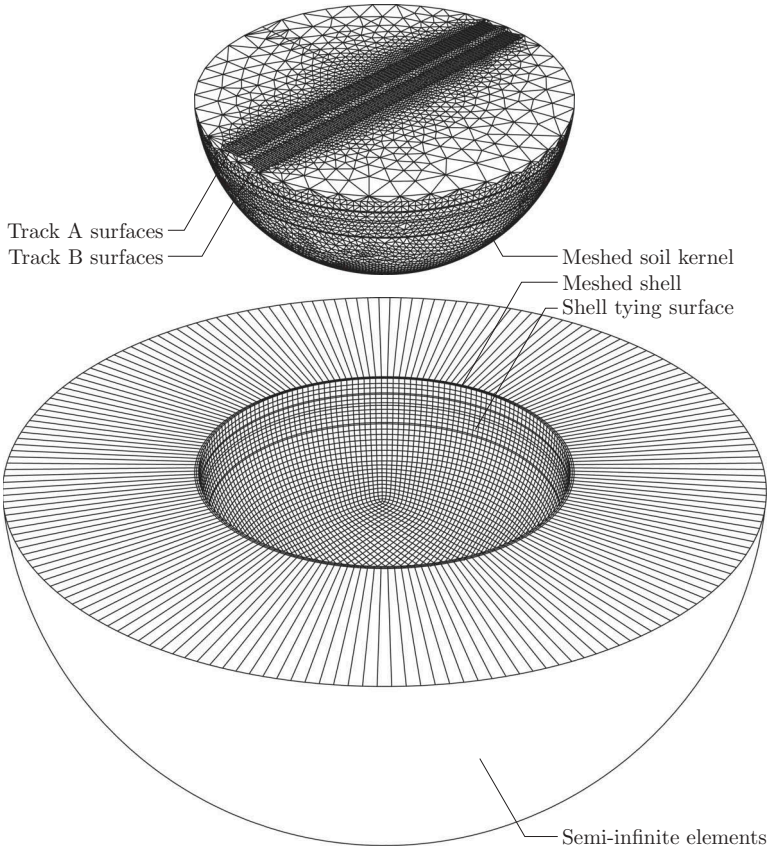

Figure 3. Representation of the soil modeling simulated in ABAQUS. The soil is composed of a solid meshed hemispherical kernel and an envelope of semi-infinite elements.

to the diameter. In the considered configuration, only one track is loaded. Therefore, the excitation of the soil is slightly asymmetrical. Both tracks are represented by the print of the sleepers on the ground (tied to behave like rigid surfaces) called surfaces in Figures 2 and 3.

- The envelope: it consists of a hollow semi-infinite hemisphere of semi-infinite elements coupled to a viscous boundary [26,27]. Technically, this envelope is created by sticking semi-infinite elements and a viscous boundary to a shell meshed with brick elements. The hollow of the envelope has the exact shape of the kernel such that they can be tied together. The purpose of the viscous boundary and semi-infinite elements is to avoid the undesirable wave reflection that would happen if the external surface of the kernel was tied to a fixed surface. Moreover, the kernel can move freely inside the semi-infinite shell. However, if the soil kernel is more free and behaves more like a realistic soil, the main drawback, already pointed out by Shih et al. [28], is the presence of a rigid body motion of the kernel inside the envelope. The influence of this phenomenon can be attenuated with a proper filtering on the results.

For the soil subsystem time-integration, ABAQUS uses a HHT-α implicit scheme [29] with automatically tuned integration parameters $\alpha = -0.05$, $\beta = 0.275625$ and $\gamma = 0.55$ such that unnecessary high-frequency content is damped by the solver itself.

3.3. Coupling approach

In co-simulation or solver-coupling techniques, two or more interacting subsystems are time-integrated using different solvers and even different software packages. Due to the interaction between the subsystems, a clocked data exchange is necessary to take the coupling into account. The timestep at which the subsystems exchange data is called the 'macrotimestep' and will be denoted by the letter 'H'. For consistency purposes, this macrotimestep must be the same in all subsystems. However, each subsystem can be time-integrated between two macrotimestep while using its own (adaptive or not) timestep (called the microtimestep and denoted by the letter 'h').

While using co-simulation, it is necessary to define the scheme that corresponds to the manner in which data are exchanged and the order in which both subsystems are time-integrated. Two usual co-simulation schemes are studied, a sequential one called Gauß-Seidel scheme and a parallel one called Jacobi scheme [25,30,31]. If z represents the state variables (displacement and velocities corresponding to the degrees of freedom) of a system and u the inputs of a subsystem, it is depicted in Figure 4 that:

- In the **Jacobi** (J) scheme, the input variables $u_{v/t}$ and u_J^τ of each subsystem are directly taken from the state variables z^τ of both subsystems obtained at the end of

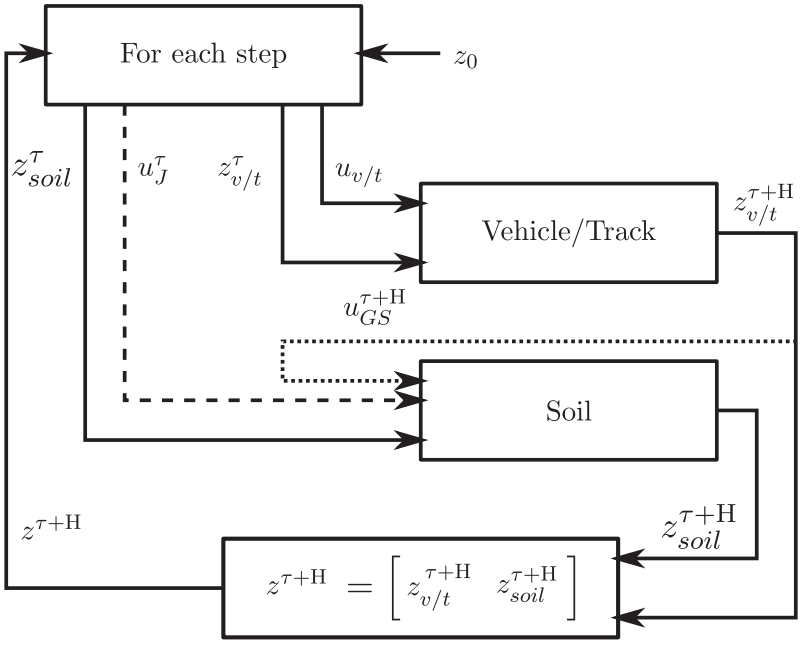

Figure 4. Gauß-Seidel scheme (dotted) – Jacobi scheme (dashed). The symbols u and z define the input and state variables respectively while τ and H represent the time and the macrotimestep respectively. v/t is the shortcut for vehicle/track subsystem.

the previous macrotimestep τ. This means that there is no communication between the subsystems during a macrotimestep and therefore the time-integration can be realized in parallel over a entire macrotimestep.

- In the **Gauß-Seidel** (GS) scheme, one subsystem is time-integrated before the other one during a macrotimestep. As for Jacobi, the input variables $u_{v/t}$ of the first subsystem being integrated are taken from the end of the previous macrotimestep τ. However, in opposition with the Jacobi scheme, the second subsystem input variables u_{GS}^{τ} are taken in the results of the aforementioned first subsystem integration in the same macrotimestep $\tau + \mathrm{H}$. This imposes to integrate a subsystem before the other one so that this scheme is, by definition, entirely sequential over a macrotimestep.

Depending on the technique used to couple two systems, the resulting coupling conditions are different. For example, some coupling techniques use algebraic constraints by literally gluing a point in both subsystems [32–35]. Another coupling technique is to consider the monolithic system split at the level of an elastic element. This has the advantage of implementing the elastic element in both subsystems so that the action of one subsystem on the other one is replaced by a force instead of an algebraic constraint. Considering this, no differential-algebraic equations are involved in the sets of equations and regular solvers can be used. This kind of coupling is called applied-force coupling [25,30]. There exist two different types of coupling when the monolithic model is split at the level of an elastic element (here the ballast). Indeed, the force developed by the elastic element has to be taken into account in both subsystems. However, this force is or is not updated during the micro-integration of each subsystem. As depicted in Figure 5 for a single spring, the two types of coupling are:

- The **displacement/displacement** coupling (denoted X-X). The elastic element, at which the split is performed, is explicitly defined in both subsystems. From the point of view of subsystem 1, the coupling force $F(z_1, \hat{z}_2)$, exerted through the

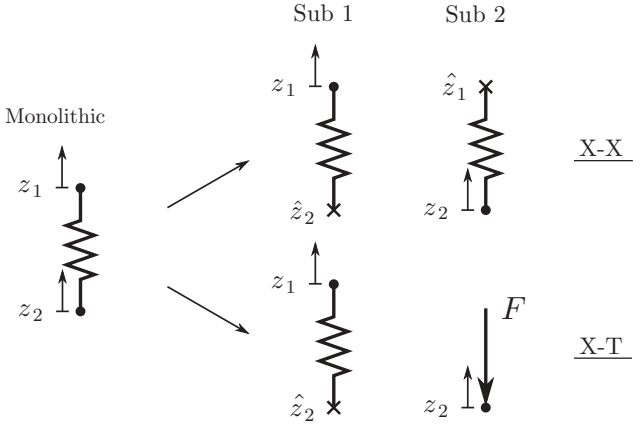

Figure 5. Difference between the displacement/displacement (X-X) and displacement/force (X-T) coupling types using a single spring element.

elastic element, directly depends on its state variable z_1 and also the coupling variable $\hat{z}_2$ coming from the other subsystem. This means that for any micro-integration between two macrotimesteps, the coupling force can be updated with respect to the state variable z_1 of the subsystem while the coupling variable $\hat{z}_2$ coming from the other subsystem remains constant over the entire macrotimestep H. The situation of the second subsystem is similar and the exerted force $F(\hat{z}_1, z_2)$ is updated only with respect to the state variable z_2 since the input variable $\hat{z}_1$ remains constant over the entire macrotimestep H.

- The **displacement/force** coupling (denoted X-T). The elastic element, at which the split is performed, is explicitly defined in one subsystem only (Sub 1 in Figure 5). This subsystem specifically receives a displacement $\hat{z}_2$ of the coupling point from the other subsystem and updates the force $F(z_1, \hat{z}_2)$ with respect to its state variable z_1 during its own micro-integrations. Meanwhile, the second subsystem receives an already computed force $F(\hat{z}_1, \hat{z}_2)$ computed in the first subsystem. This means that this force remains constant over all the micro-integrations of this second subsystem.

The constant values of the state variables $\hat{z}_1$ and $\hat{z}_2$ at time τ are the estimation of the state variables at time τ or $\tau + \mathrm{H}$ depending on the co-simulation scheme chosen. Furthermore, it has to be remarked that, when the elastic element that couples both subsystems presents also damping, the velocity of the coupling point has to be taken into account. Indeed, when a subsystem is supposed to receive a displacement and not a force, the velocity of the coupling point must be exchanged as well so that the damping effect of the coupling element can be computed.

The coupling type retained for the model presented in this work is the displacement/force one. For the sake of clarity, Figure 6 focuses on one coupling point of the displacement/force coupling type used in the vehicle/track/soil modeling. In this Figure, $q_{g,i}$ denotes the vertical displacement of the coupling surface i, $\dot{q}_{g,i}$ its vertical velocity and $F_{\text{sleeper,i/soil,i}}$ the force applied by sleeper i on soil coupling surface i.

Considering the ballast characteristics, the force involved in this specific case is given by Equation (2) in which $\mathbf{q}_g$ represents the vector containing the vertical displacement of the coupling surfaces laying on the ground.

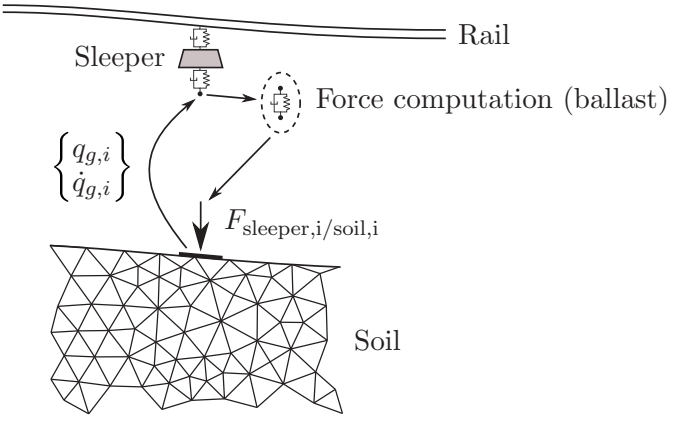

Figure 6. Focus one coupling point of the model proposed.

$$\mathbf{f}_{\text{soil/sleepers}} = k_b\left(\mathbf{q}_g - \mathbf{q}_s\right) + d_b\left(\dot{\mathbf{q}}_g - \dot{\mathbf{q}}_s\right) \tag{2}$$

From the point of view of the vehicle/track subsystem, the displacement and velocity vectors $\mathbf{q}_s$ and $\dot{\mathbf{q}}_s$ of the sleepers are part of its state variables while the displacement and velocity vectors $\mathbf{q}_g$ and $\dot{\mathbf{q}}_g$ of the ground are the inputs from the soil subsystem. Since the inputs coming from the soil ($\mathbf{q}_g$,$\dot{\mathbf{q}}_g$) subsystems are fixed during the macrotimestep, the force vector is updated through the state variables $\mathbf{q}_s$ and $\dot{\mathbf{q}}_s$ only. From the point of view of the soil subsystem, the force vector $\mathbf{f}_{\text{soil/sleepers}}$ constitutes the input from the sleepers and is directly applied on the coupling surfaces. This vector stays constant over an entire macrotimestep.

The actual implementation of the co-simulation between EasyDyn and ABAQUS deserves some more explanations. It is especially true for the finite element software for which it is necessary to comply with available features in terms of inter-process communication.

It is evident that the wall clock time required to integrate each subsystem over a macrotimestep will not be identical. Therefore, when both subsystems are integrated in parallel in the Jacobi scheme, the first subsystem whose integration finishes first has to wait for the second subsystem to be integrated to perform the data exchange. Moreover, in Gauß-Seidel scheme, it is imperative to integrate one subsystem before the other one. In any case, the implementation of data exchange between both ABAQUS and EasyDyn requires a master that will orchestrate the time-integration in such a way that it obeys to the Jacobi or the Gauß-Seidel co-simulation schemes. This master is implemented in EasyDyn since the open-source character of an in-house program offers more liberty. Moreover, the master should be able to exchange the data between the subsystems and then between the environments. Thus, the master launches a TCP/IP server and ABAQUS communicates with the latter as a TCP/IP client. Therefore, since each program launches its own threads, the EasyDyn master program controls the behavior of the communication between the server and client with respect to the data management to make it either sequential or parallel depending on the scheme chosen.

Figure 7 depicts the workflow of each software and the developed interface that allows co-simulation in between. The ABAQUS part is directly inspired by its guide for subroutines 'Writing User Subroutines with ABAQUS' in which additional information about the software workflow can be found [36]. The most important information in Figure 7 lies in the so-called interface part. Indeed, it can be seen that the master of the co-simulation process (main function of EasyDyn thread) starts a TCP/IP server that will manage the data exchange and the vehicle/track subsystem integration while ABAQUS manages the soil integration on its own. In practice, the loads required for the integration under ABAQUS are defined through the UAMP subroutine, which retrieves the data from the server.

Besides Figures 7 and 8 depicts the workflow interaction between both software packages. Typically, the following steps are involved during the time-integration:

(0) **Step 0 – Initialization**

ABAQUS side: The input file corresponding to the soil subsystem definition is read by ABAQUS. In this input file, it is specified that the loads are defined by an amplitude (ABAQUS modeling property allowing a time definition of the force). This amplitude is

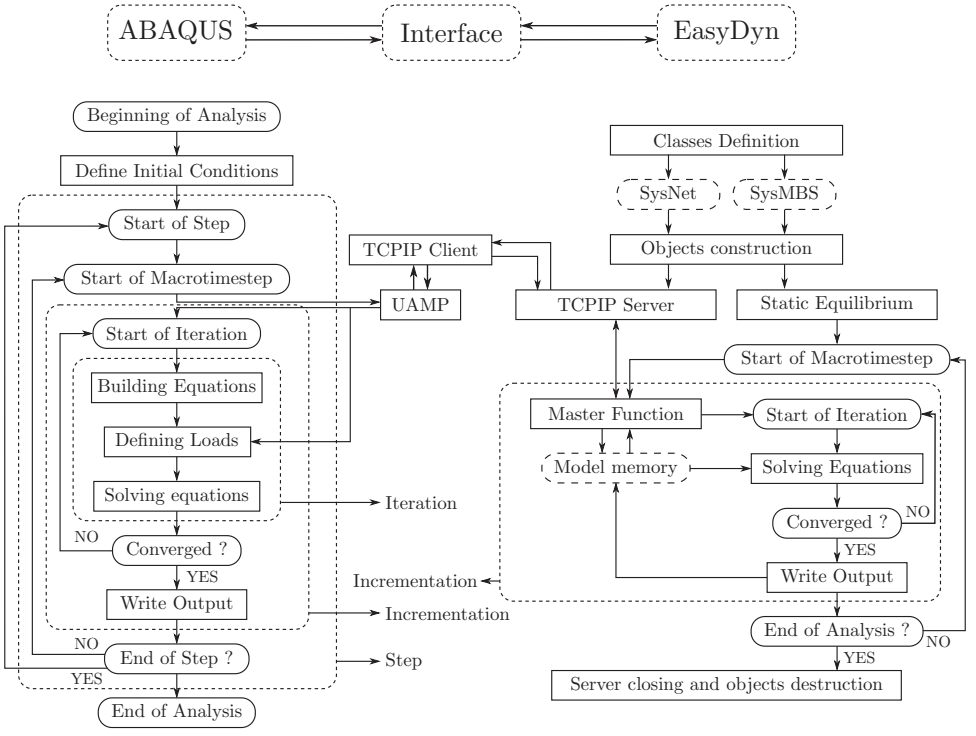

Figure 7. Interface between ABAQUS and EasyDyn workflows during co-simulation. A rectangular box depicts an action or a function call performed during the process, a rounded box depicts a decision and a dashed box represents an object or an associated property. The dashed boxes embracing other several boxes show the composition of the steps in the analysis.

user-defined using the UAMP subroutine written in C++ and pre-compiled (using a conventional C++ compiler) before the simulation launch. ABAQUS links this subroutine when the simulation begins.

EasyDyn side: The C++ code modeling the vehicle and the track is compiled and linked. The object containing the model is built and the TCP/IP server is started in a same process. The knowledge of the displacement and velocities of the soil coupling surfaces is mandatory to compute the forces developed through the ballast. From now, EasyDyn enters a waiting phase and listens to incoming TCP/IP requests.

(1) **Step 1 – Data exchange**

ABAQUS side: The UAMP subroutine calls a TCP/IP client that makes a request to the server started in EasyDyn. Another useful property of the UAMP subroutine is the ability to extract information from user-defined sensors measuring the vertical displacements and velocities of the coupling surfaces. Once the client/server connection is established, the displacements/velocities data are sent to the server. From this point, the simulation workflow of the soil enters a pause phase until the server answers the request with the force values.

EasyDyn side: The server is waiting for an incoming request. Once a client request is received, the server wakes up and receives the displacements/velocities data from the

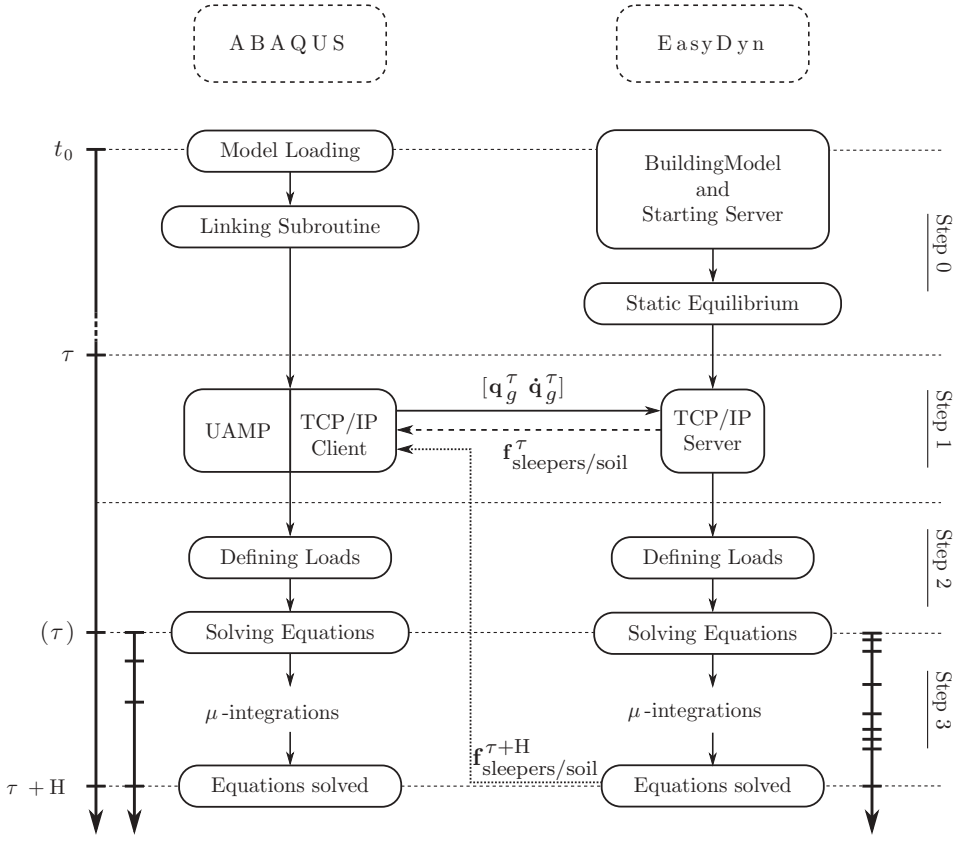

Figure 8. ABAQUS and EasyDyn workflows interaction during co-simulation.

soil subsystem. From now, EasyDyn can follow two paths depending on the simulation scheme chosen:

- *Jacobi*: Since the forces $\mathbf{f}^{\tau}_{\text{sleepers/soil}}$ have already been computed for the previous macrotimestep (time τ) in the vehicle/track subsystem, the server can send them to the client waiting on the ABAQUS side.
- *Gauß-Seidel*: The forces $\mathbf{f}^{\tau+\text{H}}_{\text{sleepers/soil}}$ exerted at the next macrotimestep are not available yet. Therefore, the server cannot immediately answer the request sent by the client and performs the following steps until it can compute the forces and send their values to the client.

(2) **Step 2 – Loads definition**

ABAQUS and EasyDyn: Either for Jacobi or Gauß-Seidel, once the coupling data are received (displacement/velocities for EasyDyn and forces for ABAQUS), the loads are defined and the equations are built. It must be mentioned that this step will be performed simultaneously for both subsystems if the Jacobi scheme is chosen. However, for Gauß-Seidel, it cannot be performed at the same time since the client in ABAQUS is still waiting for the force answer.

(3) **Step 3 – Interval**

ABAQUS side: The subsystem is time-integrated from time τ to $\tau + \mathrm{H}$ using its own microtimestep h. From this point, the macrotimestep was performed and the next one restarts from step 1.

EasyDyn side: As for the ABAQUS side, once the equations of motion are built, the macrotimestep interval H is performed using an internal microtimestep. However, depending on the method chosen in point 2, EasyDyn acts differently:

- *Jacobi*: Immediately after the time-integration, it gives the control back to the server and restarts the steps from step 1.
- *Gauß-Seidel*: Once the vehicle/track subsystem is time-integrated, the values of the forces $\mathbf{f}^{\tau+\mathrm{H}}_{\mathrm{sleepers/soil}}$ are sent to the soil subsystem through the client/server link. From now, the soil subsystem can stop its waiting phase started in step 1 and continues steps 2 and 3. Meanwhile, EasyDyn gives the control back to the server (return to step 1) and starts a waiting phase during the soil subsystem time-integration.

Figure 9 summarizes the difference between Jacobi and Gauß-Seidel workflows during a macrotimestep H. In this Figure, $\mathrm{S_i}$ represents the aforementioned step i.

4. Results

In order to validate the principles used to build the model including co-simulation, an equivalent two-step model is used as a reference. The different characteristics of the vehicle and track subdomains are given in Table 1. The vehicle/track subsystem and the vehicle/track/CLM step in the co-simulated and the two-step model are both defined in EasyDyn but are, as expected, fundamentally different. However, the soil modeling remains exactly the same in both models. The only difference, that does not lie in the modeling, concerns the forces exerted by the track on the soil. The two step model uses

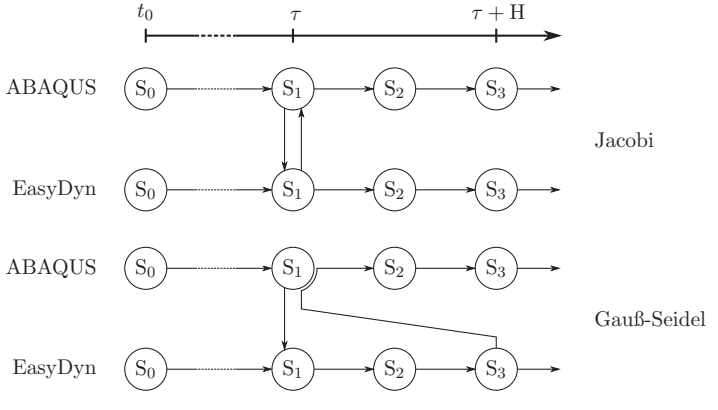

Figure 9. Difference between Jacobi and Gauß-Seidel schemes for the interaction between ABAQUS and EasyDyn workflows during co-simulation.

Table 1. Parameters defining the vehicle/track subsystem (from [37]).

Component	Parameter	Symbol	Value	Unit
Vehicle	Mass	m_v	10	T
	Speed	v_0	300	km/h
Contact	Contact stiffness	k_{Hz}	92.86	GN/m
Rail	Section	A_r	63.8	cm^2
	Geometrical moment of inertia	I_r	1987.8	cm^4
	Young's modulus	E_r	210	GPa
	Density	ρ_r	7800	kg/m^3
	Number of rail elements per sleeper	$n_{r/s}$	2	–
Railpads	Stiffness	k_p	180	MN/m
	Damping	d_p	28	kNs/m
Sleeper	Number of sleepers in start zone	$n_{s,start}$	10	–
	Number of sleepers in coupling zone	$n_{s,CS}$	81	–
	Number of sleepers in end zone	$n_{s,end}$	10	–
	Mass	m_s	90.84	kg
	Spacing	L_s	0.6	m
Ballast	Stiffness	k_p	25.5	MN/m
	Damping	d_p	40	kNs/m

a table of amplitudes while the co-simulated model uses a user-defined amplitude through a user subroutine.

The comparison between the results will be performed using three different types of the common homogeneous soil: a soft, a medium and a stiff soil distinguished by their Young modulus E of 10, 155 and 750 MPa respectively. The other characteristics defining the soils are the Poisson's coefficient $\nu = 0.25$, the viscous damping $\beta = 0.0004$ s and the density $\rho = 1540$ kg/m^3. They are considered as constant over the three soil types. The equivalent CLM reduced parameters are given in Table 2.

In the following lines and Figures, the two-step model will be denoted TS^a and the co-simulated models with Gauß-Seidel and Jacobi schemes will be denoted GS^a and J^a respectively. The superscript of each abbreviation indicates the macrotimestep as $H = 10^a$.

Figure 10 shows the magnitude of the displacements at time $t = 0.5$ s. Figure 10(a,c,e) represent the results, for the three soil types, obtained using the co-simulated model with Gauß-Seidel scheme with a macrotimestep of $H = 10^{-3}$ s. Figure 10(b,d,f) represent the

Table 2. Parameters defining the homogeneous CLM reduced soil for two-step method, from [23].

Soil type	Parameter	Symbol	Value	Unit
Soft	Lumped mass	m_f	94	kg
	Uncoupled stiffness	k_f	5	MN/m
	Uncoupled damping	d_f	180	kNs/m
	Coupling stiffness	k_c	15	MN/m
	Coupling damping	d_c	−30	kNs/m
Medium	Lumped mass	m_f	758	kg
	Uncoupled stiffness	k_f	69	MN/m
	Uncoupled damping	d_f	1120	kNs/m
	Coupling stiffness	k_c	157	MN/m
	Coupling damping	d_c	−218	kNs/m
Stiff	Lumped mass	m_f	1396	kg
	Uncoupled stiffness	k_f	317	MN/m
	Uncoupled damping	d_f	2550	kNs/m
	Coupling stiffness	k_c	724	MN/m
	Coupling damping	d_c	−300	kNs/m

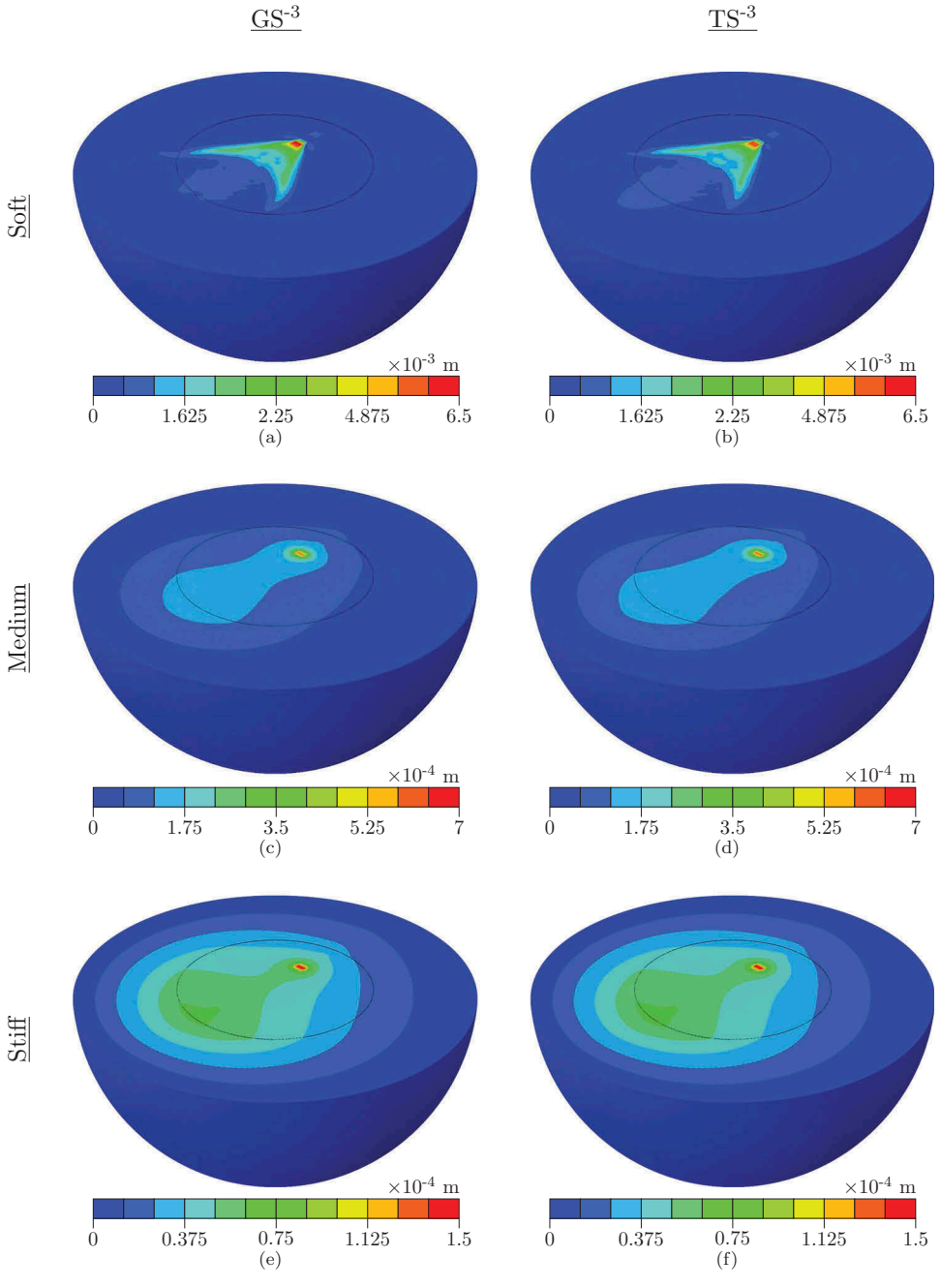

Figure 10. Magnitude of the displacements at time $t = 0.5$ s.

results obtained for the two-step model with the same macrotimestep. Visually speaking, the magnitude of the displacements obtained using the two-step model and the model using Gauß-Seidel scheme look really similar when compared on a similar scale. However, a slight difference can still be spotted in the soft soil case. Furthermore, the stiffer the soil is, the less the difference can be noticed.

Figure 11 provides the time history of the force applied a half vehicle (since the modeling is two-dimensional) on the three-dimensional soil while passing over the sleeper located in the middle of the track. Figures 11(a,b) illustrate the force for a soil with a Young Modulus E of 10 MPa, Figure 11(c,d) for a soil with $E = 155$ MPa and Figure 11(e,f) for a soil with $E = 750$ MPa. For each case, the difference between the left and the right is a focus on a different scale on the results. In those Figures, the two-step, the Jacobi and the Gauß-Seidel methods were used with a macrotimestep of H$= 10^{-3}$ s. However, since the results of J^{-3} present instability, a macrotimestep of H$= 10^{-4}$ s was used in order to compare stable results. Figures 12 and 13 are similar to Figure 11 but with the vertical displacement and the vertical velocity respectively.

It can be seen on these Figures that the results provided by the model that uses co-simulation are similar to the results obtained by the equivalent two-step modeling. However, it can be noticed that the difference becomes larger when the flexibility of the soil increases. If this phenomenon is less observable in Figure 11 that depicts the coupling force applied on the soil, it is clearly visible in Figures 12 and 13 at the displacement and velocity levels.

Since the Jacobi co-simulation scheme uses, for each macrotimestep, the values of the coupling variables obtained at the end of the previous timestep while Gauß-Seidel uses an updated version of those values for the second subsystem integration, it can be imagined that Jacobi will involve a deeper loss of accuracy than Gauß-Seidel. This loss of accuracy can lead to an amplification of the error accumulation and then generate, in some cases, instability. Figures 11–13 (soft soil results only) clearly show that Jacobi can lead to an instability while Gauss-Seidel stays stable for a same macrotimestep and a same soil configuration. Moreover, theoretically speaking, the loss of accuracy is a function of the chosen macrotimestep [25] and should then decrease when the macrotimestep decreases as well. If the macrotimestep tends towards 0, Jacobi and Gauss-Seidel should converge to the same solution. Moreover, decreasing the macrotimestep sometimes lead to stable results. Both phenomena are visible on the aforementioned Figures.

In Figure 14, the wall clock time required on the same computer (AMD FX-tm 8350 4.0 GHz) to perform the simulation is given for the two different timesteps H$= 10^{-3}$ s and H$= 10^{-4}$ s (Figure 14(a,b) respectively). The J^{-3} simulation is not represented since the simulation was unstable and failed. It can be seen that the soil type does not really affect the simulation time while the type of model chosen does. Generally speaking, for the microtimestep H$= 10^{-3}$ s, Jacobi is the fastest and Gauß-Seidel the slowest with the two-step model in between. Since Jacobi is parallel and both software packages actually run simultaneously while Gauß-Seidel stays sequential, the difference between the simulation time of both co-simulation schemes is due to the fact that the time-integration of the vehicle/track subsystem is hidden behind the soil subsystem one. Since the two-step model is also, a fundamentally sequential process, it is normal that the Jacobi scheme remains faster. The fact that the Gauß-Seidel simulation time is bigger than the time of the two-step model could be explained by the time required for the data exchanges and a less efficient convergence in the vehicle/track subsystem due to the loss of accuracy provoked by the co-simulation process.

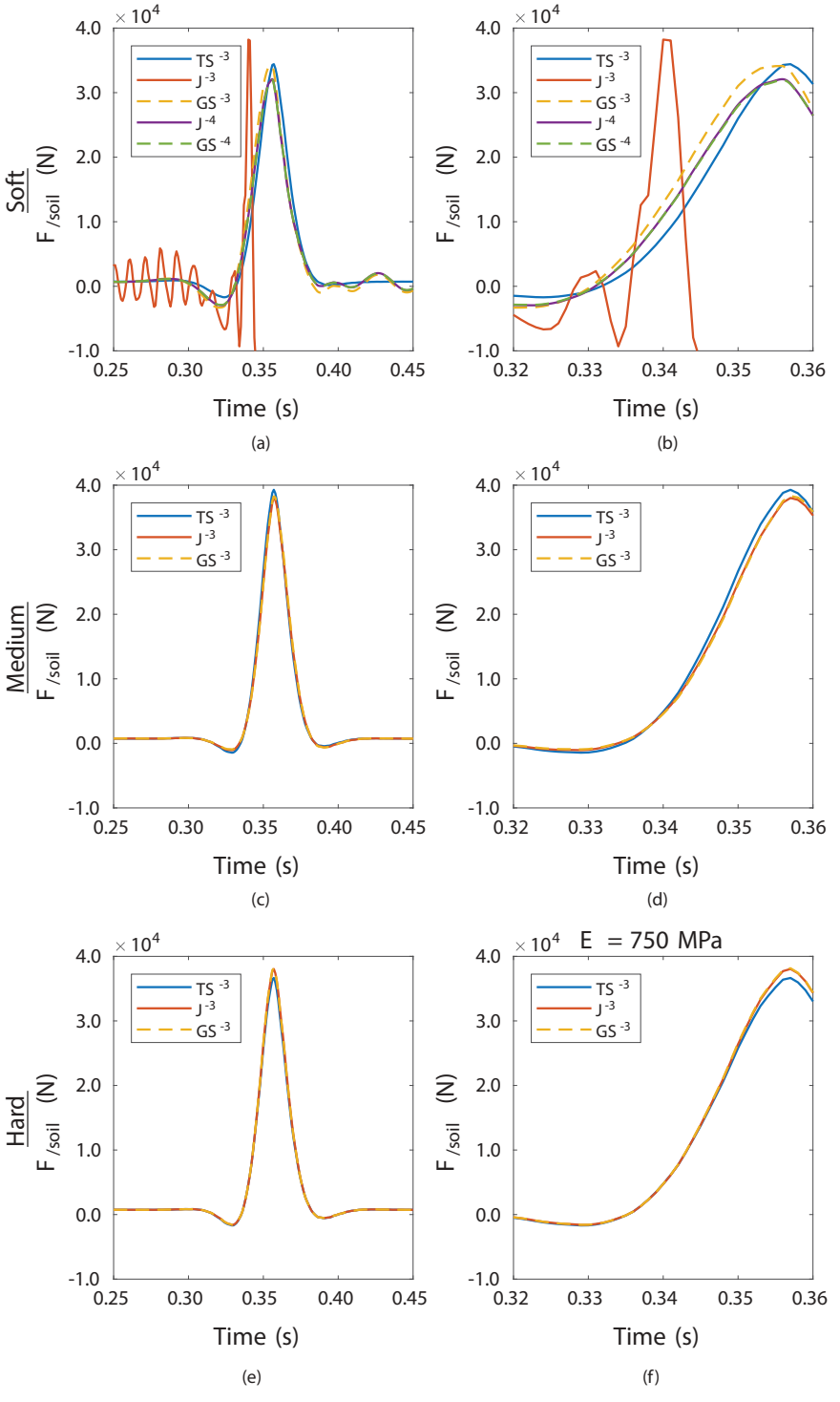

Figure 11. Time history of the force applied by one side of the vehicle on the soil while passing over the sleeper located in the middle of the track. (left: focus on the wheel passage, right: zoom on the incoming situation).

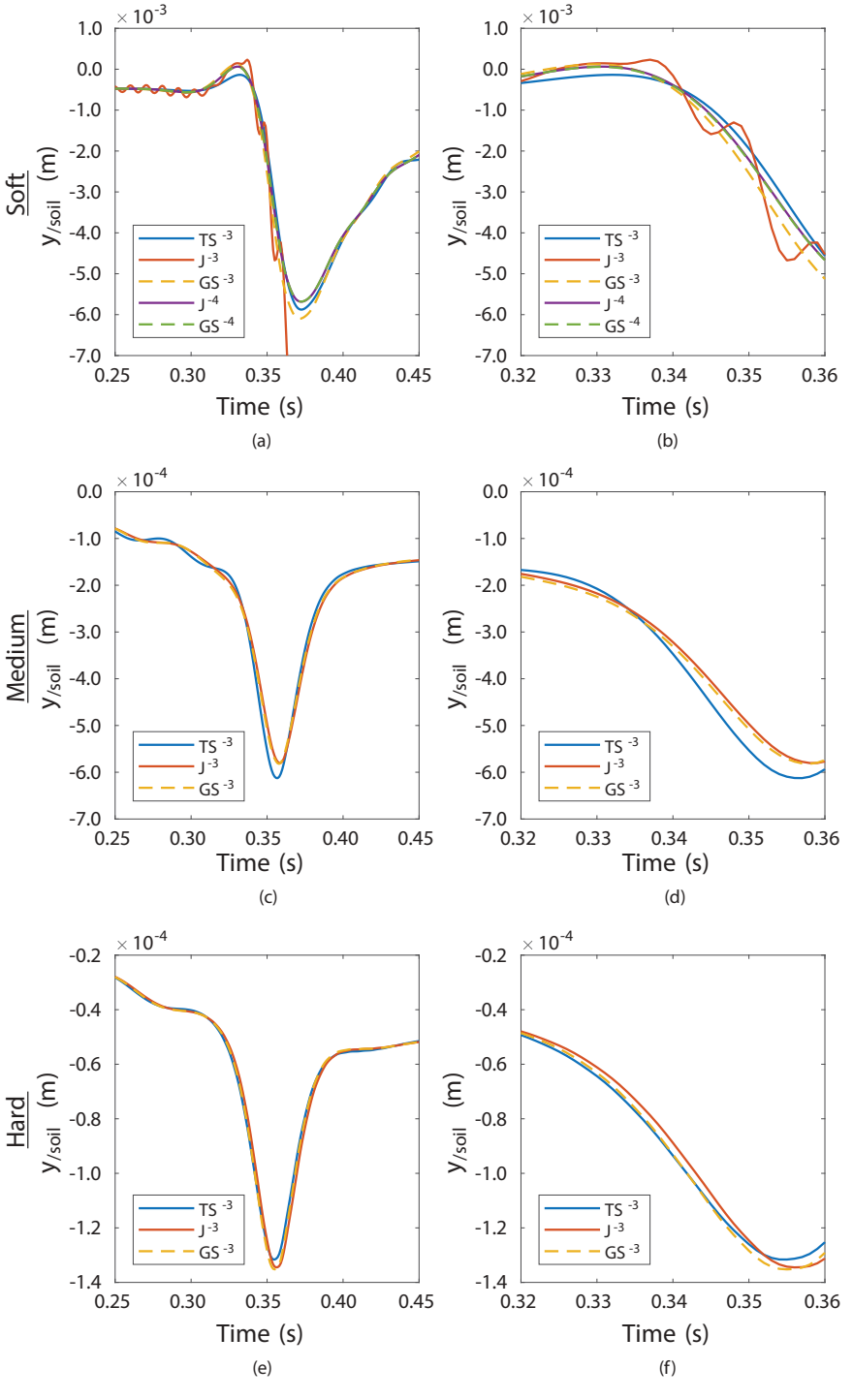

Figure 12. Time history of the vertical displacement of the soil surface located in the middle of the track. (left: focus on the wheel passage, right: zoom on the incoming situation).

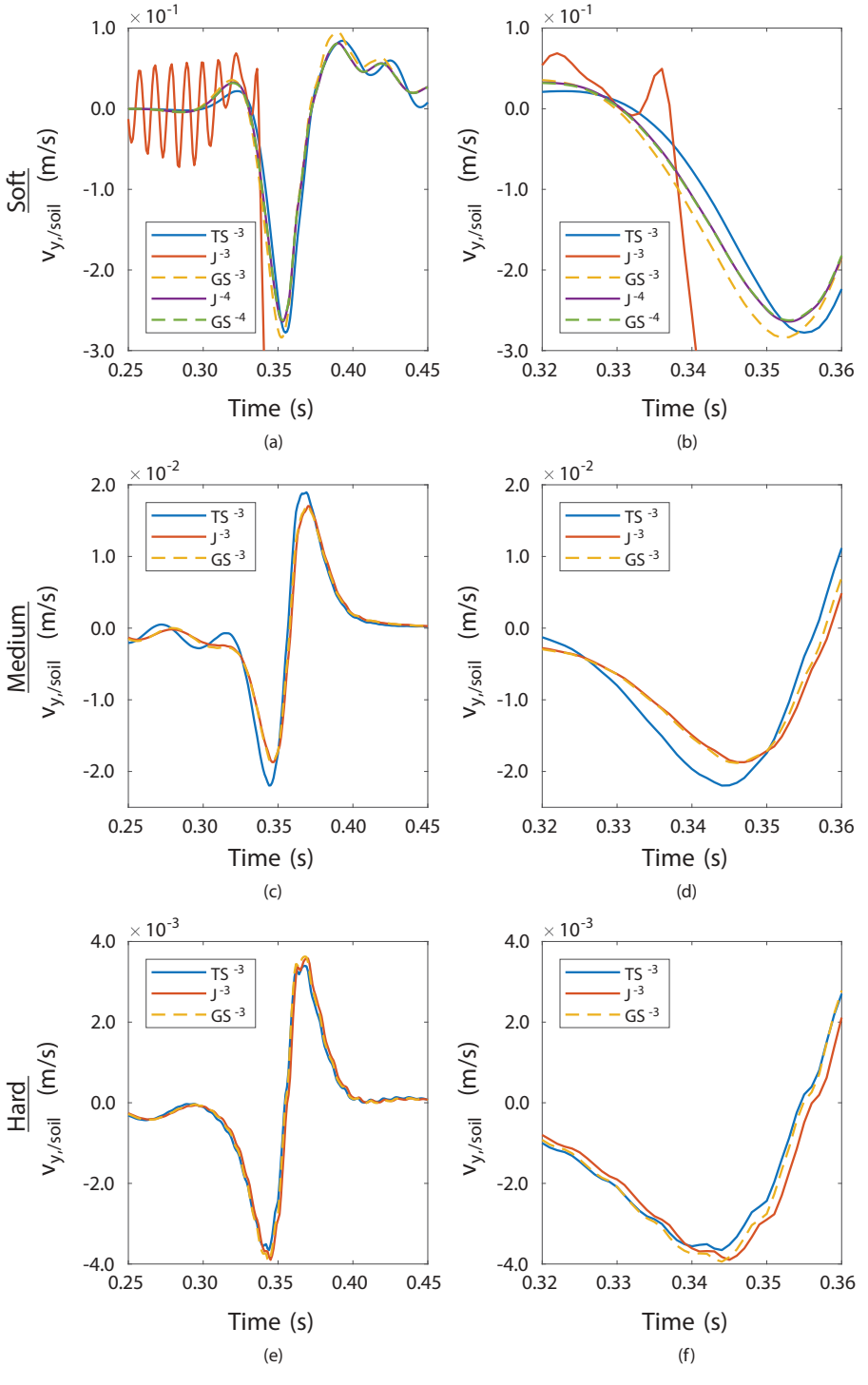

Figure 13. Time history of the vertical velocity of the soil surface located in the middle of the track. (left: focus on the wheel passage, right: zoom on the incoming situation) .

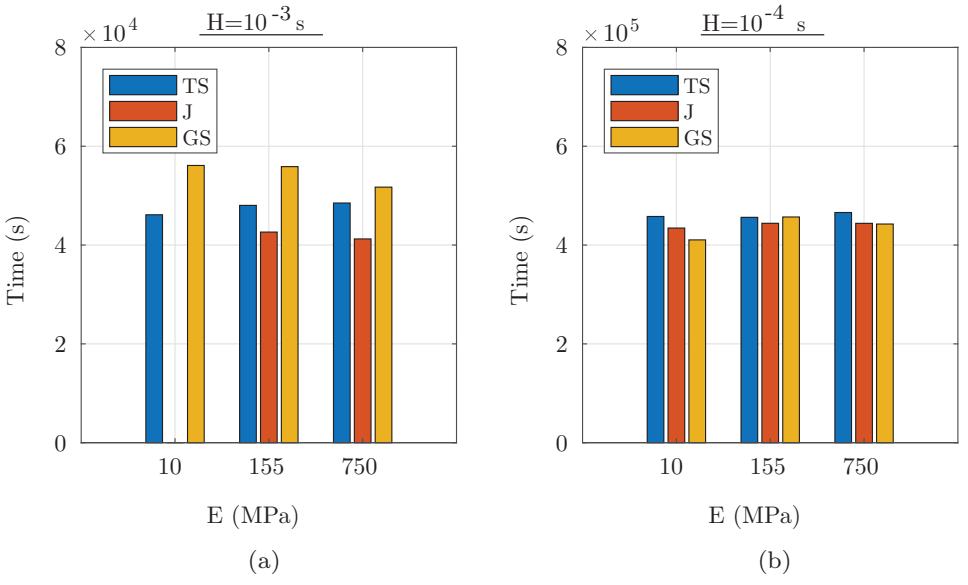

Figure 14. Wall clock time required for the different simulations.

Figure 14(b) also shows that when the macrotimestep decreases, the difference in the simulation time becomes negligible. A reasonable hypothesis to explain this phenomenon could be the adaptive microtimestep of the solver used in the vehicle/track subsystem. Indeed, this microtimestep is adaptive in order to reach a certain order of accuracy. Therefore, even if the macrotimestep is defined at $H = 10^{-3}$ s, smaller timesteps are still investigated in the vehicle track subsystem while the linear definition of the soil converges in only one iteration. Therefore, in the case of a macrotimestep of $H = 10^{-4}$ s, the time required for the integration of the soil subsystem could become dominating.

5. Conclusions

Two co-simulation schemes, a sequential one and a parallel one, were presented to build a model that couples a vehicle/track subsystem and a soil subsystem. From the point of view of the nature of the problem, this co-simulated model remains similar to a two-step model that is used as a reference to compare the results obtained with. The major differences between the two-step model and the co-simulated model lied in two points:

- The sequence of subdomains integration: in the two-step model, the vehicle and track subdomains are completely integrated over time before the soil subdomain while, in the co-simulated model, all subdomains are integrated with continuous interaction.
- The presence of a reduced model of the soil in the vehicle and track step integration in the two-step model: this reduced model of the soil is no more necessary in the co-simulated model since both subsystems communicate during the integration process.

The working process of a connection, specifically developed to couple an open-source in-house software and a commercial software, was detailed. This connection allows bilateral communication between the two considered subsystems through the management properties of the TCP/IP protocol. Moreover, the data management used provided the practical implementation of both sequential and parallel co-simulation schemes.

The similarity between two-step and co-simulated models was demonstrated through the comparison of the coupling forces acting between both vehicle/track and soil subsystems as well as the displacement and the velocities of the coupling surfaces. Furthermore, it was also evoked that the macrotimestep and the co-simulation scheme used have a capital influence in terms of stability and accuracy of the solution obtained. Moreover, the difference between the parallel and the sequential co-simulation schemes was highlighted. Indeed, the integration of one subsystem is hidden behind the other one in the Jacobi scheme. This provides a computational time lower than in the Gauß-Seidel case and also lower than the two-step simulation time. However, if the parallel scheme is faster, it was shown that it is also the less stable in a similar situation. This lack of stability is essentially due to the explicit characteristic of the co-simulation schemes used. In addition, the parallel scheme will, by definition, use a less accurate estimation of the inputs for the second subsystem integration than in the sequential case. This phenomenon reinforce the lack of stability in the Jacobi scheme. Furthermore, attention should be paid to the intrinsic solver of each subsystem since one solver could become dominating and then balance the simulation time between both parallel and sequential coupling schemes.

Finally, besides the similarity between the two-step and the co-simulated models, the mechanism of co-simulation provides interesting advantages:

- In order to estimate the forces applied on the soil in the second step of the two-step model, an accurate CLM reduction of the soil is required. The parameters of this CLM soil can also be determined iteratively. Using co-simulation, no reduction of the soil is required since both subsystems are directly coupled during the integration process.
- Moreover, if the soil is not homogeneous or if there exist some complex structures nearby the track, the co-simulation process directly takes into account the effect of these additional features.
- Furthermore, in a more practical way, the co-simulated model proposed in this paper allows a separated modeling of both vehicle/track and soil subsystems if the input and output data of both subsystems are known. This could be highly interesting for a company in terms of confidentiality or even in terms of project management.

Disclosure statement

No potential conflict of interest was reported by the authors.

ORCID

Bryan Olivier http://orcid.org/0000-0002-4170-3883

Georges Kouroussis http://orcid.org/0000-0002-9233-1354

References

[1] Iwnicki S. Handbook of railway vehicle dynamics. CRC press; 2006.
[2] Knothe K, Wu Y. Receptance behaviour of railway track and subgrade. Arch Applmech. 1998;68(7–8):457–470.
[3] Newmark NM. A method of computation for structural dynamics. J Eng Mech Div. 1959;85(3):67–94.
[4] Chung J, Hulbert GM. A time integration algorithm for structural dynamics with improved numerical dissipation: the generalized-α method. J Appl Mech. 1993;60 (2):371–375.
[5] Bazzi G, Anderheggen E. Theρ-family of algorithms for time-step integration withimproved numerical dissipation. Earthquake Eng Struct Dyn. 1982;10(4):537–550.
[6] Zhai W, He Z, Song X. Prediction of high-speed train induced ground vibration based on train-track-ground system model. Earthquake Eng Eng Vibr. 2010;9(4):545–554.
[7] Wang L, Zhu Z, Bai Y, et al. A fast random method for three-dimensional analysis of train-track-soil dynamic interaction. Soil Dyn Earthq Eng. 2018;115:252–262.
[8] Fernández Ruiz J, Alves Costa P, Calçada R, et al. Study of ground vibrations induced by railway traffic in a 3D FEM model formulated in the time domain: experimental validation. Struct Infrastruct Eng. 2017;13(5):652–664.
[9] Gardien W, Stuit H. Modelling of soil vibrations from railway tunnels. J Sound Vib. 2003;267(3):605–619.
[10] Nielsen J, Lombaert G, François S. A hybrid model for prediction of ground- borne vibration due to discrete wheel/rail irregularities. J Sound Vib. 2015;345:103–120.
[11] Yang J, Zhu S, Zhai W, et al. Prediction and mitigation of train-induced vibrations of large-scale building constructed on subway tunnel. SciTotal Environ. 2019;668:485–499.
[12] Song X, Li Q. Numerical and experimental study on noise reduction of concrete LRT bridges. SciTotal Environ. 2018;643:208–224.
[13] Kouroussis G, Zhu S, Olivier B, et al. Urban railway ground vibrations induced by localized defects: using dynamic vibration absorbers as a mitigation solution. J Zhejiang Univ Sci A. 2019;20(2):83–97.
[14] Olivier B, Connolly DP, Alves Costa P, et al. The effect of embankment on high speed rail ground vibrations. Int J Rail Trans. 2016;4(4):229–246.
[15] Connolly D, Giannopoulos A, Forde M. Numerical modelling of ground borne vibrations from high speed rail lines on embankments. Soil Dyn Earthq Eng. 2013;46:13–19.
[16] Wu Q, Spiryagin M, Cole C, et al. Parallel computing in railway research. Int J Rail Trans. 2018. in press:1–24. DOI:10.1080/23248378.2018.1553115
[17] Wu Q, Sun Y, Spiryagin M, et al. Parallel co-simulation method for railway vehicle-track dynamics. J Comput Nonlin Dyn. 2018;13(4):041004.
[18] Antunes P, Magalhães H, Ambrósio J, et al. A co-simulation approach to the wheel–rail contact with flexible railway track. Multibody Sys Dyn. 2019;45(2):245–272.
[19] Dietz S, Hippmann G, Schupp G. Interaction of vehicles and flexible tracks by co-simulation of multibody vehicle systems and finite element track models. Veh Syst Dyn. 2002;37(sup1):372–384.
[20] Verlinden O, Fékih LB, Kouroussis G. Symbolic generation of the kinematics of multi-body systems in EasyDyn: from MuPAD to Xcas/Giac. Theor Appl Mech Lett. 2013;3 (1):013012.
[21] Dassault Systèmes - Simulia. ABAQUS 6.13 Documentation. 2013.
[22] Kouroussis G, Van Parys L, Conti C, et al. Using three-dimensional finite element analysis in time domain to model railway-induced ground vibrations. Adv Eng Software. 2014;70:63–76.

[23] Kouroussis G, Gazetas G, Anastasopoulos I, et al. Discrete modelling of vertical track–soil coupling for vehicle–track dynamics. Soil Dyn Earthq Eng. 2011;31(12):1711–1723.
[24] Nielsen JCO, Abrahamsson TJS. Coupling of physical and modal components for analysis of moving non-linear dynamic systems on general beam structures. Int J Numer Method Biomed Eng. 1992;33(9):1843–1859.
[25] Olivier B, Verlinden O, Kouroussis G. Chapter 12, Stability and error analysis of applied- force co-simulation methods using mixed one-step integration schemes. In: Schweizer B, editor. IUTAM bookseries 35. Cham: Springer; 2019. p. 1–12. doi:10.1007/978–3–030–14883–612
[26] Lysmer J, Kuhlemeyer RL. Finite dynamic model for infinite media. J Eng Mech Div. 1969;95(4):859–878.
[27] Kouroussis G, Verlinden O, Conti C. Finite-dynamic model for infinite media: corrected solution of viscous boundary efficiency. J Eng Mech. 2011;137(7):509–511.
[28] Shih JY, Thompson DJ, Zervos A. The effect of boundary conditions, model size and damping models in the finite element modelling of a moving load on a track/ground system. Soil Dyn Earthq Eng. 2016;89:12–27.
[29] Hilber HM, Hughes TJR, Taylor RL. Improved numerical dissipation for time integration algorithms in structural dynamics. Earthquake Eng Struct Dyn. 1977;5(3):283–292.
[30] Busch M Zur effizienten Kopplung von Simulationsprogrammen. Ph.D. thesis, Kassel University. 2012.
[31] Gomes C, Thule C, Broman D, et al. Co-simulation: a survey. ACM Comput Surveys. 2018;51(3):49.
[32] Schweizer B, Li P, Lu D. Implicit co-simulation methods: stability and convergence analysis for solver coupling approaches with algebraic constraints. ZAMM - J Appl Math Mech. 2016;96(8):986–1012.
[33] Schweizer B, Lu D, Li P. Co-simulation method for solver coupling with algebraic constraints incorporating relaxation techniques. Multibody Sys Dyn. 2016;36(1):1–36.
[34] Wang J, Ma ZD, Hulbert GM. A gluing algorithm for distributed simulation of multibody systems. ASME 2003 International Design Engineering Technical Conferences and Computers and Information in Engineering Conference: Volume 5: 19th Biennial Conference on Mechanical Vibration and Noise, Parts A, B, and C. Chicago, IL: American Society of Mechanical Engineers; 2003. p. 89–104.
[35] Rustin C, Verlinden O, Bombled Q A cosimulation T-T procedure gluing subsystems in multibody dynamics simulations. ASME 2009 International Design Engineering Technical Conferences and Computers and Information in Engineering Conference: Volume 4: 7th International Conference on Multibody Systems, Nonlinear Dynamics, and Control, Parts A, B and C. San Diego, CA: American Society of Mechanical Engineers; 2009. p. 83–92.
[36] Dassault Systèmes - Simulia. Abaqus 6.13 User Subroutines Reference Guide. 2013.
[37] Kouroussis G, Verlinden O, Conti C. Influence of some vehicle and track parameters on the environmental vibrations induced by railway traffic. Veh Syst Dyn. 2012;50(4):619–639.